



An IoT Integrated Air Quality Monitoring Device Based on Microcomputer Technology and Leading Industry Low-Cost Sensor Solutions

Ioannis D. Apostolopoulos¹(✉), George Fouskas¹, and Spyros N. Pandis^{1,2}

¹ Foundation for Research and Technology Hellas – Institute of Chemical Engineering Sciences, Patras, Greece

japostol@iceht.forth.gr

² Department of Chemical Engineering, University of Patras, Patras, Greece

Abstract. Indoor and outdoor air quality monitoring is essential for the prevention of undesired exposure to air pollutants, especially for sensitive groups. Extensive exposure to particulate and gaseous pollutants can cause temporary and chronic respiratory and other diseases and even lead to premature death. The emergence of low-cost sensors enables the development of affordable devices that measure the concentrations of various pollutants and notify humans for the quality of the air that they breath. Current microcomputer technology and the advances in wireless communications, as well as data systems, provide space for Internet of Things devices that monitor, track, store and analyze pollutant concentration measurements enabling data analytics. In this work, we describe the development and testing of a compact, integrated air quality monitoring device that detects and reports fine particulate matter (PM_{2.5}), nitrogen dioxide (NO₂), and ozone (O₃) levels as well as temperature (T) and relative humidity (RH).

Keywords: Air quality monitoring · Internet of Things · Low-cost sensors · Calibration · Microcomputers · Raspberry PI

1 Introduction

In recent years, the monitoring and reporting of indoor and outdoor Air Quality (AQ) have become an urgent need [1]. Real-time monitoring can provide many benefits. For example, accurate knowledge of the level of air quality in a city can provide warnings for sensitive groups and also lead to mitigation actions to reduce the respiratory and other problems caused by the high air pollutant concentrations [2, 3].

Breathing particulate matter can cause premature death especially in people with heart or lung disease, aggravated asthma, decreased lung function, and increased respiratory symptoms, such as irritation of the airways, coughing or difficulty breathing [4]. Exposure to ozone has been found to trigger a variety of health problems, such as

chest pain, coughing, throat irritation, and congestion [4, 5]. Nitrogen dioxide aggravates respiratory symptoms, increases hospital admissions, and emergency department visits, particularly in asthmatics, children, and older adults; increases susceptibility to respiratory infection [6].

Traditional monitoring and reporting the exact concentrations of pollutants require high costs. Accurate instruments are quite expensive and it is difficult to have tens of measurement stations even in a large city [7]. Precision air pollution measurement instruments can cost from a few tens of thousands of euro to hundreds for a complete measurement suite [1].

In recent years, several new micro-sensors for monitoring and recording the concentrations of particles and gaseous pollutants have been developed. These sensors have low-cost but they are less accurate than traditional air quality monitors. Low-cost sensors have attracted the interest of many institutes, scientific bodies and researchers, as well as companies [8–10]. Despite their disadvantages, such as measurement uncertainty, frequent errors, periods of instability, etc. [11], these sensors offer a new approach for high spatial resolution air quality monitoring (AQM) in urban areas in both the developed and the developing world.

A plethora of projects have employed various low-cost sensors to characterize air quality. For example, RAMP (SENSIT Technologies), is a device that can measure various gas pollutants, such as ozone, nitrogen dioxide, nitrogen monoxide, carbon monoxide, as well as particulate matter (PM_{2.5} and PM₁₀) and carbon dioxide [12]. The RAMP has been evaluated in several research projects in urban, indoor, and industrial environments [12–14]. A low-cost device dedicated to particulate matter (PM_{2.5} and PM₁₀) concentration measurement has been developed by PurpleAir and it intended for both indoor and outdoor use. Studies have shown that this particular device is an effective solution the measurements of fine particulate matter levels [15, 16]. AEROQUAL is another device developed for monitoring several gaseous pollutants and meteorological conditions [17].

In this work, we present an AQM solution, which offers stability, accuracy, and ease of use. Leveraging the capabilities of microcomputers and the Internet of Things (IoT), we propose a smart indoor and outdoor AQM device equipped with efficient, cutting-edge low-cost sensors, which are selected based on recent research and evaluation campaigns. The device is based on the Raspberry PI microcomputer, which operates on top of the analog and digital sensors and is responsible for sensor data acquisition, storage and transmission. It also offers a variety of device monitoring services, such as network connectivity configuration. Low-cost sensors, such as Plantower PMS5003, Alphasense NO₂-B43F and Alphasense OX-B431, are used to estimate the concentration of fine particulate matter (PM_{2.5}) and the two major gaseous pollutants (NO₂, O₃). Henceforth, this device is referred to as ENvironment SENSIng Appliance (ENSENSIA).

The overall contributions of the present work can be summarized as follows:

1. We present a low-cost AQM solution for indoor and outdoor environments
2. The proposed device is evaluated in real conditions against another well-established low cost device (RAMP)

3. ENSENSIA enables real-time parameter tuning for remote control and intelligent edge-computing implementation of linear corrections to the raw readings. The coefficients of the linear regression can also be tuned remotely
4. A functional and user-friendly platform is developed for visualizing the sensor's readings

2 Materials and Methods

2.1 Hardware

Raspberry PI Microcomputer. ENSENSIA relies on the newest Raspberry Pi Model 4B. Raspberry PI is a low-cost, credit-card sized computer that operates like a normal personal computer. Its small size enables its use in several environments and aids to its transferability. Raspberry PI Model 4B includes 4 USB ports, 2 mini-HDMI ports for screen display, as well as Ethernet port. Raspberry PI functionalities can be extended by leveraging the 40-pin headers, which allow for integrating several handcrafted or commercial Hardware Attached on Top (HAT). HATs are expansion boards that connect to the Raspberry Pi's set of 40 GPIO pins and add multiple functionalities, such as sensors, fans, 4G transmitters and more.

UPS. Falling voltages and long power outages can affect the operation of the device. Therefore, a UPS HAT was implemented to maintain the power supply. Waveshare UPS HAT uses I2C bus communication and offers real-time monitoring of battery voltage, current, power, and remaining capacity. This HAT integrates multi-battery protection circuits, such as discharge and over-charge protection.

2.2 PMS5003 Sensor

PMS5003 is a matchbox-sized particulate matter (PM) sensor that reports PM concentrations for various size ranges (including $PM_{2.5}$ and PM_{10}). It is based on laser technology under the light scattering principle to obtain its readings. PMS5003 has been examined and evaluated by several research studies [12, 18, 19] and stands out to be an excellent solution for low-cost AQM projects. Its characteristics are summarized in Table 1.

The PMS5003 performance for fine PM ($PM_{2.5}$) has been found to be very good under most conditions, while its ability to measure coarse particles (in the 2.5–10 μm diameter range) appears to be problematic [10]. Therefore, it will only be used for $PM_{2.5}$ measurements in the proposed device.

Table 1. PMS5003 sensor specifications

Specification	Value/description
Sensor type	Dust sensor – laser technology
Typical input voltage	4.5–5.5 V DC
Operating current	100 mA
Communication protocol	UART, TTL Serial
Power consumption in work mode	Below 100 mA
Sensitivity	50% – 0.3 μm , 98% – 0.5 μm and larger
Working temperature	–10 to 60 °C
Working relative humidity range	0–99%

2.3 Alphasense NO2-B43F Sensor

Alphasense sensors have been used in several AQM projects [20–22]. The US Environmental Protection Agency (EPA) is occasionally evaluating such sensors in ambient collocation setups, offering variety of reports that demonstrate reliability, accuracy, and precision. NO2-B43F is designed to measure nitrogen dioxide (NO₂) levels. The specifications of the sensor are summarized in Table 2.

Table 2. NO2-B43F sensor specifications

Specification	Value/description
Sensor type	Electrochemical NO ₂ sensor
Typical input voltage	5 V DC
Communication protocol	Analog
Sensitivity	–220 to –650 nA/ppm at 2 ppm NO ₂
Working temperature	–30 to 40 °C
Working relative humidity range	15–85%

2.4 Alphasense OX-B431 Sensor

Similar to the NO2-B43F sensor, OX-B431 is designed to measure ozone concentrations. It works in conjunction with NO2-B43F. The specifications of the sensor are summarized in Table 3.

The performance of OX-B431 has been also evaluated in several studies [23, 24] and has been found to be acceptable under specific environmental conditions.

Table 3. OX-B431 sensor specifications

Specification	Value/description
Sensor type	Electrochemical O ₃ sensor
Typical input voltage	5 V DC
Communication protocol	Analog
Sensitivity	−225 to −750 nA/ppm at 2 ppm O ₃
Working temperature	−30 to 40 °C
Working relative humidity range	15–85%

2.5 BME680 Sensor

BME680 (Bosch Sensortec) integrates temperature, humidity, and pressure sensors [25]. Its size and low-power consumption make it a good choice for portable devices and wearables. Its specifications are summarized in Table 4. BME680 has been evaluated in several studies and has been found to be one of the best options for the specific task [26, 27].

Table 4. BME 680 sensor specifications

Specification	Value/description
Sensor type	Meteorological
Typical input voltage	1.7–3.6 V DC
Communication protocol	I ² C and SPI
Working conditions	Temperature: −40 to 85 °C Humidity: 0 to 100% Pressure: 300 to 1100 hPa

2.6 PCB Development

All sensors operate via the SDA-SCL and RTX-TDX channels of the Raspberry PI, allowing for I²C and SPI connectivity/communication protocols. The complete board is furnished with male and female pin-headers to host the sensor chips and ensure a stable card for their operation. To this end, a PCB has been developed and is illustrated in Fig. 1.

PCB is designed using the open-source software KICAD.

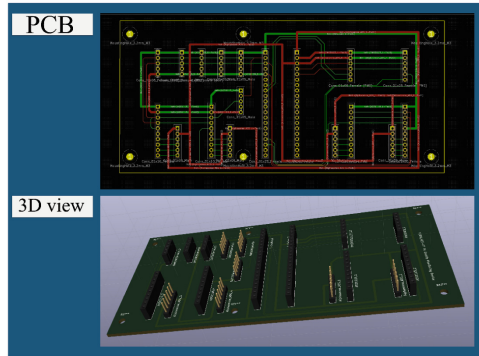


Fig. 1. PCB design.

2.7 Packaging of AQM Device

ENSENIA should operate without interruptions in various environmental conditions. Meanwhile, it is required to be of minimum size to increase its portability. Air pollutant sensors are exposed to ambient conditions and should be protected from wind gusts, rain, and dust. Therefore, we have designed a box for the device that meets these criteria (Fig. 2). The sensors are placed at the bottom of the box, in special holes that isolate the electronic parts of the sensor from the inlets from which the air to be measured enters.

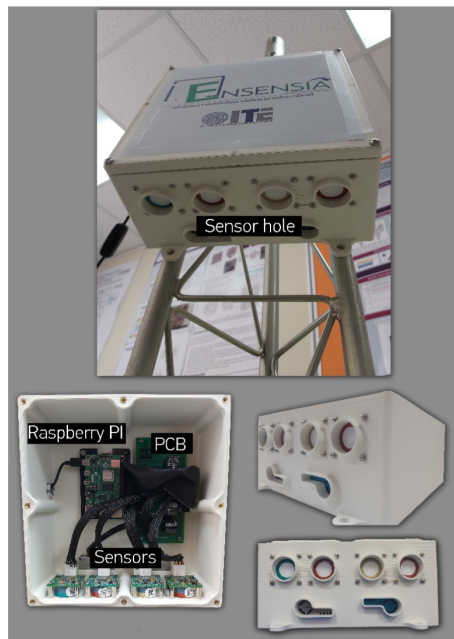


Fig. 2. The complete AQM device.

Around the edges of the sensor, and at a depth slightly greater than the depth of the exposed surface of the sensor, a plastic shield is placed. For further protection from living organisms, the surfaces of the sensors are protected by a special screen.

The box is designed to the specifications of a waterproof (IP65-66), durable and lightweight material and is manufactured via a 3D printer (Leapfrog – Bolt PRO). Figure 2 illustrates the inside and the outside of the ENSENSIA device.

2.8 Software

Raspberry PI Firmware, Internet and Functions. Raspberry PI’s operational system is the official Raspberry PI OS. Raspberry PI consists of an integrated Wi-Fi-module and supports an Ethernet cable connection. For the specific project, the device is configured to use a Wi-Fi connection. ENSENSIA operates within a Python Programming language framework (version 3.8). All configurable parameters are stored in a special file with an.ini extension. This file is read from the python scripts to adjust the corresponding tunable parameters in real-time.

MQTT Protocol. Data-centric communication is a new paradigm used in Wireless Sensor Networks (WSN). One form of data-centric communication examples is that of publish/subscribe messaging system that is dominant in distributed computing. MQTT is a topic-based protocol, based on publish/subscribe method [28]. MQTT uses character strings and enables the subscription to multiple topics. MQTT requires a client to setup a connection with a broker [28]. Both client and broker need to stay connected to a specific topic to exchange messages. Messages are not stored in any format with this communication protocol. Hence, a client publishing a message to a topic that a broker is not listening will be lost. The broker supervises the liveness of the client/connection by a “keep-alive” timer, which defines the maximum time interval that may elapse between two messages received from that client.

We have used the Mosquitto [29] open-source implementation of MQTT protocol to enable such communication between the server and ENSENSIA.

Server-Side Data Processing and Storage (MariaDB). Messages published by the client (AQM device) are processed by a python script that operates on the server side and establishes an MQTT connection between the broker and the clients. The decoded messages are appropriately interpreted into useful measurements that are stored in a local database. We use MariaDB server for such operations, which is a popular and effective open-source relational database. MariaDB is furnished by the developer of MySQL and is the default database server for most Linux distribution systems. The sensor readings are organized into separate MySQL tables.

Alarms. Alarms play essential role in modern IoT applications [30]. They are designed to notify the user about a specific situation where a malfunction or an undesired event took place. ENSENSIA is configured to track and monitor its condition and inform the server about several critical factors that affect its AQM effectiveness. PCB and sensor I/O errors, abnormal sensor readings (such as peaks) and system-focused information, such as CPU temperature and available SD card memory space, are communicated with

the server every 2 min. In this way, the user can have a complete overview of what is happening inside the device and can prevent potential malfunction.

Parameter Tuning and Real-Time Calibration. Remote parameter tuning is highly desirable in IoT devices and provides flexibility, transferability, and ease-of-use. The proposed AQM device supports remote parameter tuning in a secure way by leveraging the capabilities of MQTT.

ENSENSIA uses the MQTT protocol to mirror its current state in the server at a prefixed time interval (default is every 30 s). The server is listening to the MQTT messages from the device and is storing the device's current state in an SQL table. A second SQL table is utilised to store the desired state, which is defined by the remote user. A Python script operating on the server-side is responsible for comparing the two tables and generating the necessary messages back to the AQM device. Real time correction of the raw measurements is enabled by remotely tuning the coefficient a and the residual b of the linear correction formula based on the sensor calibration:

$$Measurement_{corrected} = a(Measurement_{raw}) + b \quad (1)$$

In this way, the user can change if needed the calibration equation of the device effortlessly to correct for errors, such as over-time drift. The user can also manually place the device under zero air conditions and adjust the parameters to correct the sensor readings. Use of other more complex correction equations and algorithms is possible if needed.

2.9 Visualization

NetData Cloud. Inspection of ENSENSIA's real-time performance in terms of system operations is an essential feature of modern IoT devices. Netdata is a distributed platform that provides real-time performance and health monitoring of sensor devices, especially the ones operating with the Raspberry PI technology. The Netdata agent is free and open-source and comes with the Netdata cloud agent, which provides various visualizations for monitoring the system's activity.

Netdata collects thousands system, hardware and application metrics and utilizes approximately 1% of the CPU to offer this service. It is also endowed with hundreds of default alarms that are fully customizable.

Real-Time Air Quality Monitoring Visualizations. The ENSENSIA device comes with a specially designed web interface platform providing useful gauges, graphs, charts and forms to visualize the air quality and the device's functions. Those services are summarized in Table 5.

The web interface is developed using open-source software and is hosted by the Informatics and Communication Centre of the Institute of Chemical Engineering Sciences in Patras, Greece. Figure 3 illustrate some examples.

Table 5. Web interface utilities

Interface/page	Utilities
Gauges	Provides gauges for visualizing the sensor readings
Charts	Provides charts to illustrate historical sensor data
Status	Informs the user of the current status of the devices (online/offline)
Configuration	Enables remote parameter tuning
Alarms	Presents a set of pre-defined alarms
Map	Places each associated sensor on a map, where the user can inspect the locations of the sensors and access their current readings

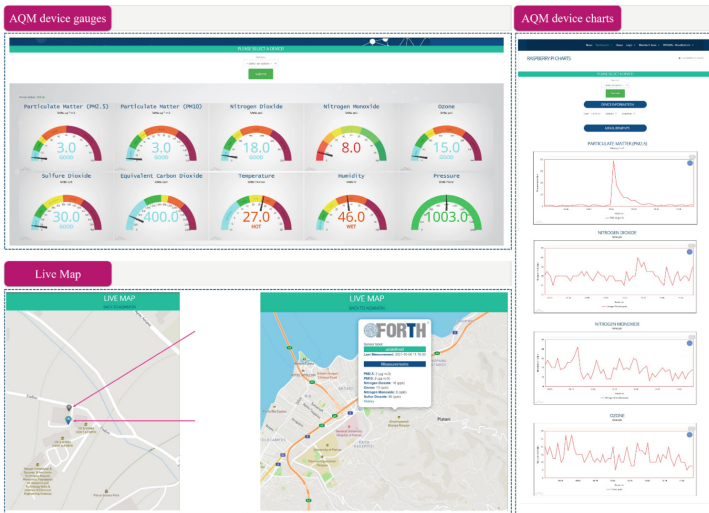


Fig. 3. Web interface (2)

2.10 Device Evaluation Co-location Setups

ENSENSIA has been tested in the field after co-location with established low-cost AQM systems (RAMP). In this way, the proposed AQM device is evaluated for its effectiveness compared to its counterpart, which is considered to be a stable and reliable low-cost AQM device. In this section, we provide descriptions of the measurement sites, the associated infrastructure and the experimental setups.

Measurement Sites. FORTH/ICE-HT ambient

The devices were placed on the roof of the institute’s facilities, which is in a suburban area, about 5 km from the city of Patras, a city of approximately 300,000 inhabitants. The exact location of the site is at a latitude of 38.2979 and a longitude of 21.8090. The site is about 3 km from the coast.

FORTH/ICE-HT indoor

The AQM device was placed inside an office of the ICE-HT institute which contains three desks and several servers. During the campaign, there were on average two persons in the office during the working hours of 8 am to 4 pm.

Collocation Setups (CS). Preliminary evaluation setups are designed and performed to inspect the performance of the developed AQM device (Table 6). Indoor and outdoor performance was examined using other instrumentation next to RAMP. Inter-unit consistency tests were also conducted. Inter-unit consistency is an important test prior to evaluation with reference measurements. For the purposes of the campaign, a second identical ENSENSIA device was developed to inspect the response of both devices, when placed together under the same conditions.

Table 6. AQM device evaluation campaigns.

CS #	Starting date	End date	Measurement site	Devices
1	30/9/2021 12:00	5/10/2021 23:00	Indoor (office)	ENSENSIA, RAMP
2	14/10/2021 10:00	20/10/2021 10:00	Outdoor	ENSENSIA, RAMP
3	1/7/2021 10:00	13/7/2021 9:00	Outdoor	2 ENSENSIA devices

CS #1 refers to a 6-day evaluation of the device's performance in indoor conditions. The device was placed in the office, as explained earlier. A RAMP was also located inside the office next to our ENSENSIA device.

CS #2, an ambient collocation setup (CS #2) was used for seven days. A RAMP was located next to the ENSENSIA device.

CS #3 was used for 13 days in ambient conditions outdoors. During this campaign, two ENSENSIA devices were collocated to investigate the inter-unit consistency. No reference instrumentation was present in this setup.

Correction. The correction formulas for $PM_{2.5}$ proposed by [10] were used for the Plantower PMS5003 measurements. These have been developed for the same urban area. The corresponding correction equation is:

$$PM_{2.5|corrected} = 0.42 * PM_{2.5|measured} + 1.26 \mu g m^{-3} \quad (2)$$

where $PM_{2.5|measured}$ is the raw measurement reported by the sensor. More complex corrections are needed for the NO_2 and O_3 concentrations [12]. For the rest of the sensor readings of both RAMP and ENSENSIA, no further calibration formulas or methods were applied. RAMP sensors, as well, as ENSENSIA sensors come factory-calibrated. The user should note that field calibration is important for low-cost sensors and requires reliable reference instrumentation. The authors intend to perform such tasks in future studies.

Evaluation Metrics. A series of evaluation metrics can be used for the quantification of the performance of low-cost sensors. The Mean Error (ME) or Mean Error (ME) and

Root Mean Squared Error (RMSE) are absolute accuracy metrics and give the average errors with respect to the reference measurements. The Normalized Mean Error (nME) is a relative accuracy metric. Finally, the Mean Bias (MB) describes the bias of the sensor compared to the reference device.

Given a set of n values (O_i) from the reference instrument and a set of values (E_i) for the low-cost sensor the above metrics are calculated using the following equations:

$$ME = \frac{\sum_{i=1}^n |E_i - O_i|}{n} \quad (3)$$

$$RMSE = \sqrt{\frac{\sum_{i=1}^n (E_i - O_i)^2}{n}} \quad (4)$$

$$MB = \frac{\sum_{i=1}^n (O_i - E_i)}{n} \quad (5)$$

$$nME = \frac{\sum_{i=1}^n |O_i - E_i|}{\sum_{i=1}^n E_i} \quad (6)$$

R (correlation coefficient) and R^2 (coefficient of determination) are correlation metrics that describe the strength of relationship between the sensor readings and the reference measurements. Studies suggest that at least ME, RMSE, R, R^2 , and nME [11] should be reported.

3 Results

3.1 Device Measurement Stability

We evaluated the stability of ENSENSIA with the following criteria: a) continuous, uninterrupted operation of the Raspberry PI device, and b) continuous, uninterrupted data flow at specific intervals (2 min). We monitored the device's battery level and data messages over a period of 30 days during July 2021. ENSENSIA is configured to transmit measurements ever two minutes. Hence, the total number of expected data packets was 21600. The received measurements were 21103 less than the expected, resulting in a data loss of 2.3%. This was mostly due to 3 power outages in the area and also to some Wi-Fi connectivity problems. There were no power outages of the Raspberry PI. The average battery charge (from 20% to 95%) time after a power outage was 4 h.

3.2 Indoor Assessment (CS #1)

The $PM_{2.5}$ concentrations during the measurement period varied from 3.75 to 10.9 $\mu\text{g m}^{-3}$ (average 6.5 $\mu\text{g m}^{-3}$). The corresponding range for NO_2 was 12–18 ppb (average 14.6 ppb) and O_3 from 2 to 18 ppb (average 9.6 ppb). The indoor evaluation metrics of ENSENSIA against the RAMP measurements are summarized in Table 7. The metrics correspond to averages of the measurements over 60 min.

Table 7. Assessment metrics for CS #1 for hourly-averaged measurements

	PM _{2.5} ($\mu\text{g m}^{-3}$)	NO ₂ (ppb)	O ₃ (ppb)	Temperature ($^{\circ}\text{C}$)	Humidity (%)
R	0.96	0.76	0.56	0.95	0.90
R ²	0.92	0.58	0.38	0.91	0.81
ME	0.39	0.91	2.04	0.38	1.75
RMSE	0.49	1.12	2.58	0.48	2.1
MB	-0.02	-0.02	-0.17	-0.25	-1.42
nME	0.1	0.07	0.09	0.02	0.01

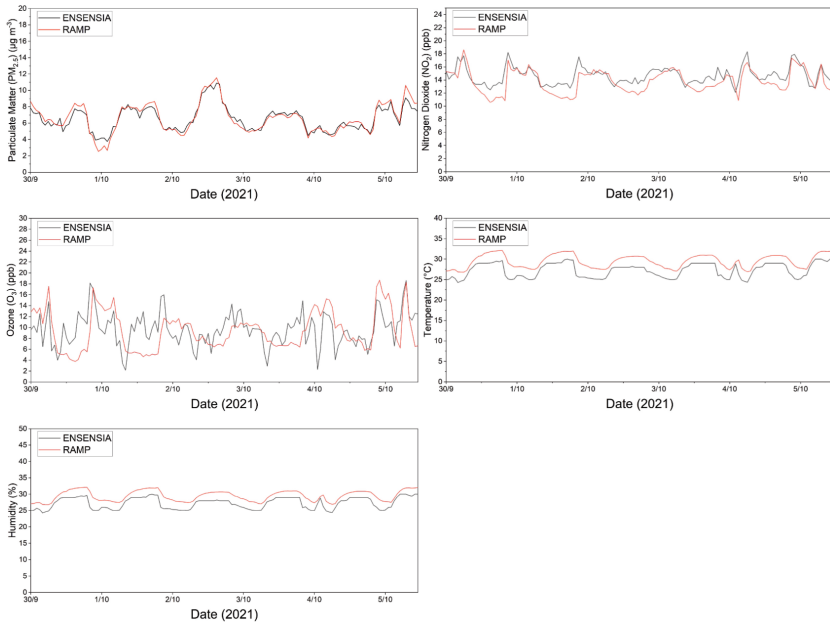


Fig. 4. Time-series for the measurements of PM_{2.5}, O₃, NO₂, T, and RH for CS #1 from the ENSENSIA device and the RAMP device.

The agreement of the ENSENSIA for PM_{2.5} was encouraging with little bias ($-0.02 \mu\text{g m}^{-3}$), high correlation ($R = 0.96$) and a RMSE of only $0.39 \mu\text{g m}^{-3}$. The normalized mean discrepancy (nME) is 1%. The two devices also gave similar NO₂ measurements with a nME of 7% and a RMSE of 1.1 ppb (Fig. 4).

The moderate correlation ($R = 0.76$) is due to a large extent to the narrow range of the concentrations during the measurements. Indoor ozone was quite low during the measurement period, but the two devices once more gave measurements consistent with each other (nME = 9%) and a RMSE of only 2.6 ppb. The meteorological sensors gave measurements with an average discrepancy of 1–2% (Fig. 5).

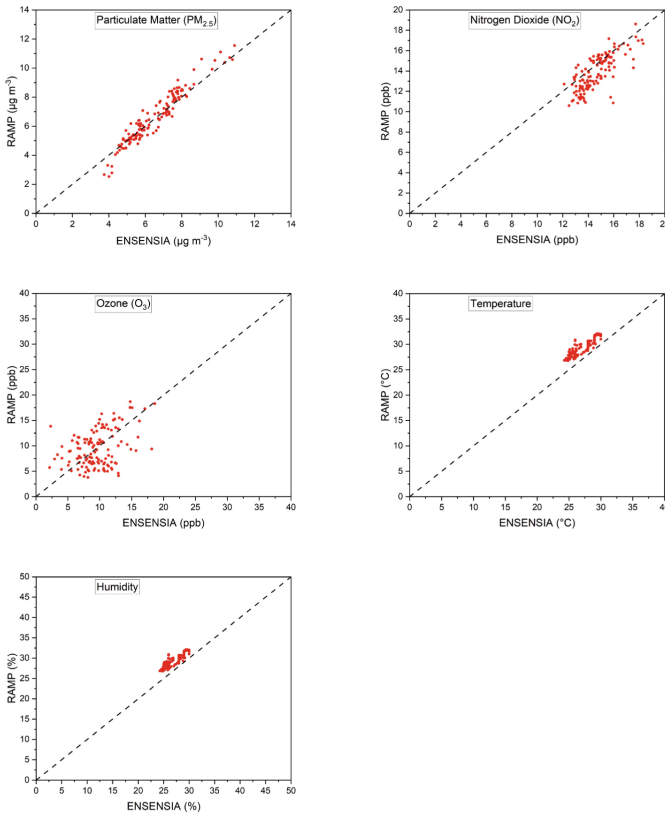


Fig. 5. Scatter plots for the measurements of $\text{PM}_{2.5}$, O_3 , NO_2 , T, and RH for CS #1.

3.3 Outdoor Assessment (CS #2)

The $\text{PM}_{2.5}$ concentrations during the measurement period varied from 2 to $23 \mu\text{g m}^{-3}$ (average $7.24 \mu\text{g m}^{-3}$). The corresponding range for NO_2 was 2–24 ppb (average 18.29 ppb) and O_3 from 2 to 60 ppb (average 29.9 ppb). The indoor evaluation metrics of ENSENSIA against the RAMP measurements are summarized in Table 8. The metrics correspond to averages of the measurements over 60 min.

The agreement of ENSENSIA for $\text{PM}_{2.5}$ showed $-0.47 \mu\text{g m}^{-3}$ bias, high correlation ($R = 0.98$) and little RMSE of $1.01 \mu\text{g m}^{-3}$. nME is found to be 6%. The two devices also yielded similar NO_2 readings ($R = 0.85$) with a nME of 11%. Ozone levels were higher compared to the indoor experiments. Again, the two devices gave consistent measurements, with a nME of 10% and RMSE of 6.86 ppb. The moderate correlation ($R = 0.71$) is a result of discrepancy between the sensors in higher concentrations, as seen in Fig. 6.

The meteorological sensors gave measurements with an average discrepancy of 1–2% (Fig. 7).

Table 8. Assessment metrics for CS #2 for hourly-averaged measurements

	PM _{2.5} ($\mu\text{g m}^{-3}$)	NO ₂ (ppb)	O ₃ (ppb)	Temperature ($^{\circ}\text{C}$)	Humidity (%)
R	0.98	0.85	0.71	0.95	0.97
R ²	0.96	0.72	0.50	0.92	0.94
ME	0.81	1.52	3.00	1.39	2.01
RMSE	1.01	2.38	6.86	2.04	2.56
MBE	-0.47	0.92	1.91	-1.33	-0.25
nMAE	0.06	0.11	0.10	0.01	0.01

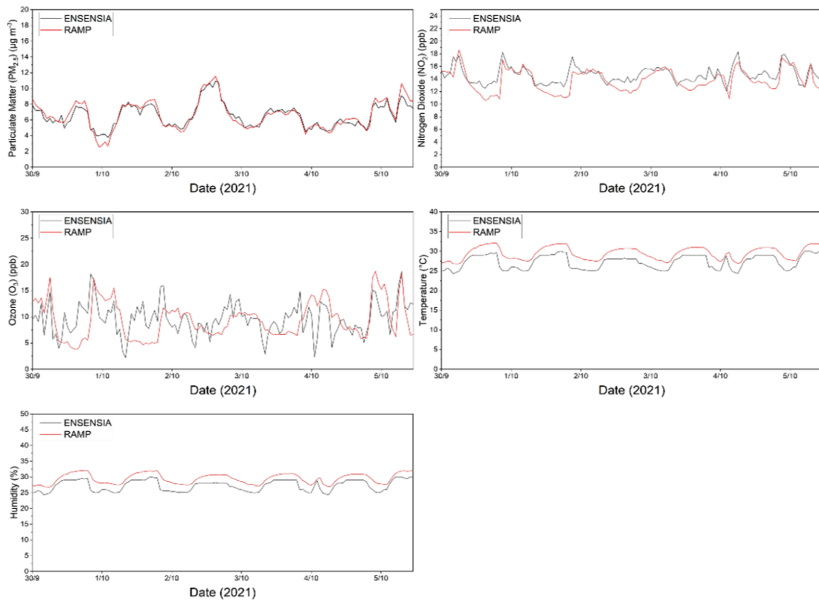


Fig. 6. Time-series for the hourly values of PM_{2.5}, O₃, NO₂, T, and RH for CS #2 from the ENSENSIA device and the RAMP device.

3.4 Inter-unit Consistency (CS #3)

Inter-unit consistency tests are conducted to validate measurement agreement between identical devices, in terms of hardware and software. Slight measurement variations are expected according to the manufacturers of the low-cost sensors. In Table 9, the evaluation metrics are presented. Assessment metrics are recorded from hourly-averaged values.

The two devices show high correlation factors among their readings. PM_{2.5}, PM₁₀, T, and RH yield a very high correlation ($R = 0.99$) and small RMSE and bias (Fig. 8).

The nME is found to be 1–2%. NO₂ and O₃ sensors show moderate correlation ($R = 0.81$ and $R = 0.84$ respectively) (Fig. 9).

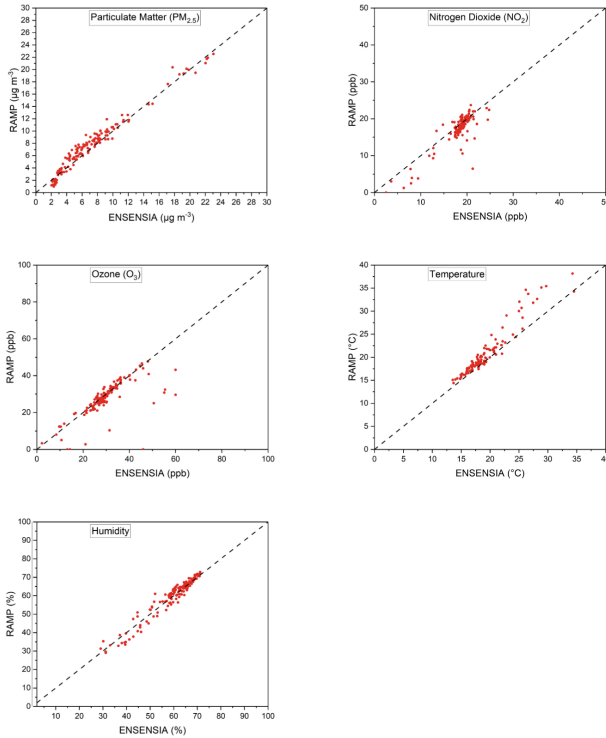


Fig. 7. Scatter-plots for the hourly values of PM_{2.5}, PM₁₀, O₃, NO₂, T, and RH for CS #2.

Table 9. Assessment metrics for CS #3 for hourly-averaged measurements

	PM _{2.5} ($\mu\text{g m}^{-3}$)	NO ₂ (ppb)	O ₃ (ppb)	Temperature ($^{\circ}\text{C}$)	Humidity (%)
R	0.99	0.81	0.84	0.99	0.99
R ²	0.98	0.62	0.71	0.97	0.98
ME	1.57	1.13	11.39	0.56	0.75
RMSE	1.77	1.80	15.21	0.56	0.91
MBE	1.53	0.76	-0.34	-0.24	-0.47
nMAE	0.02	0.16	0.03	0.02	0.01

4 Discussion and Conclusions

We presented the hardware and software components and the newly developed AQM device (ENSENSIA). The new device communicates with a user-friendly web interface that provides gauges, charts and real-time parameter tuning, as well as default alarms to monitor the device status. We evaluated ENSENSIA with respect to its operating stability, its agreement with a well-established AQM device counterpart (RAMP), and its agreement with an identical device (inter-unit consistency). Raspberry PI showed great stability during the assessment tests and proved to be a reliable low-cost solution

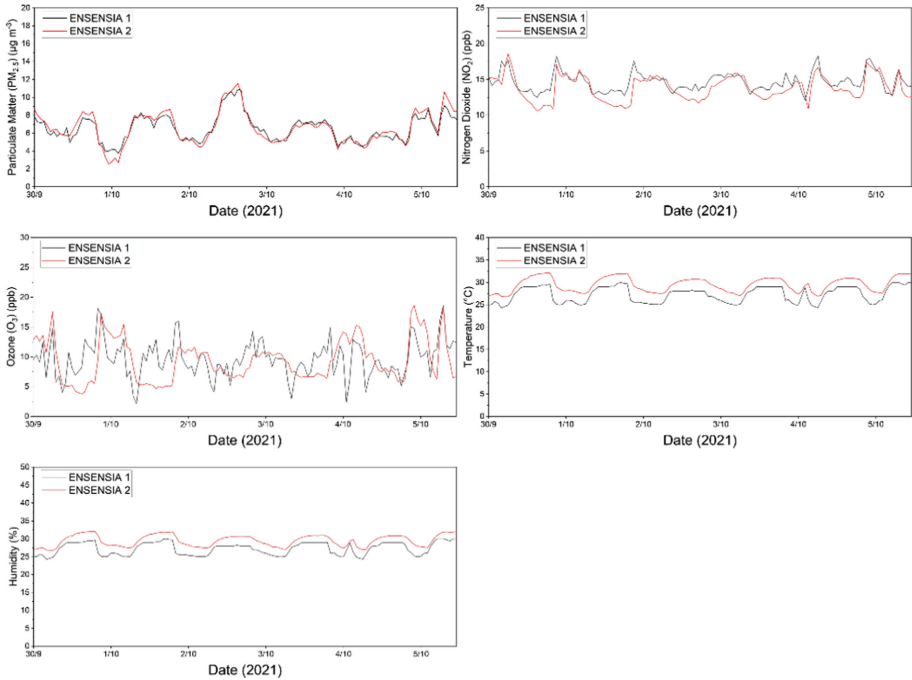


Fig. 8. Time-series for the measured and the reference hourly values of PM_{2.5}, PM₁₀, O₃, NO₂, T, and RH for CS #3.

for such AQM applications. The hourly measurements of the new device had normalized mean errors of less than 2% for PM_{2.5}, NO₂ and O₃ for both the indoor and outdoor tests compared to the established low-cost sensing RAMP system. Also, inter-unit consistency tests showed promising results. The discrepancy between the two identical units was little, as expected, and can be eliminated with the use of linear formulas that correct the bias. In the next steps of this work the new AQM device will be evaluated against reference instruments that are used for regulatory applications for much longer periods and for a much wider range of atmospheric concentrations and conditions. MQTT and web-interface security measures are already studied to limit security vulnerabilities.

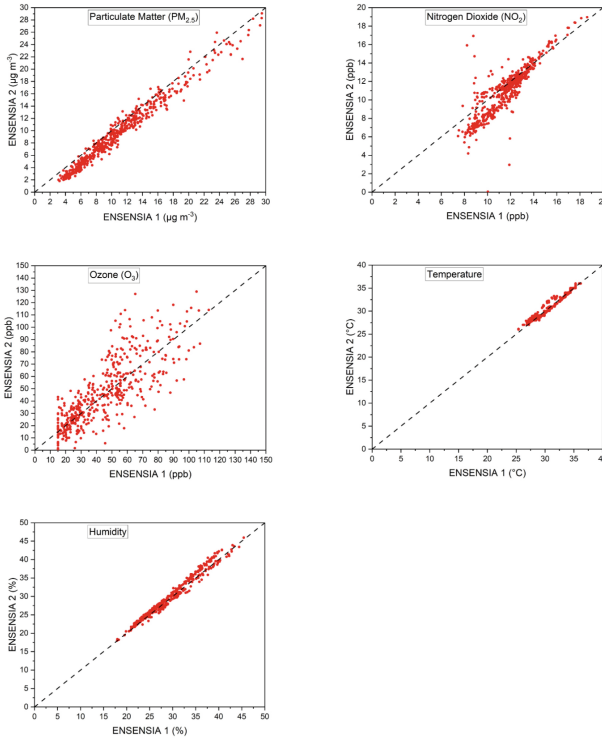


Fig. 9. Scatter-plots for the measured and the reference hourly values of PM_{2.5}, PM₁₀, O₃, NO₂, T, and RH for CS #3.

5 Conflicts of Interest

The authors declare that there are no conflicts of interest.

Funding. This work was partially supported by the “KRIPIS - Poytita Zois II” project (MIS 5002464), which has received funding the General Secretariat for Research and Innovation, Greece.

References

1. Malings, C., et al.: Fine particle mass monitoring with low-cost sensors: corrections and long-term performance evaluation. *Aerosol Sci. Technol.* **54**, 160–174 (2020). <https://doi.org/10.1080/02786826.2019.1623863>
2. Lelieveld, J., Haines, A., Pozzer, A.: Age-dependent health risk from ambient air pollution: a modelling and data analysis of childhood mortality in middle-income and low-income countries. *Lancet Planet. Health* **2**, e292–e300 (2018). [https://doi.org/10.1016/S2542-5196\(18\)30147-5](https://doi.org/10.1016/S2542-5196(18)30147-5)
3. Goldemberg, J., Martinez-Gomez, J., Sagar, A., Smith, K.R.: Household air pollution, health, and climate change: cleaning the air. *Environ. Res. Lett.* **13**, 030201 (2018). <https://doi.org/10.1088/1748-9326/aaa49d>

4. Liu, X., et al.: Low-cost sensors as an alternative for long-term air quality monitoring. *Environ. Res.* **185**, 109438 (2020). <https://doi.org/10.1016/j.envres.2020.109438>
5. Nuvolone, D., Petri, D., Voller, F.: The effects of ozone on human health. *Environ. Sci. Pollut. Res.* **25**(9), 8074–8088 (2017). <https://doi.org/10.1007/s11356-017-9239-3>
6. Atkinson, R.W., Butland, B.K., Anderson, H.R., Maynard, R.L.: Long-term concentrations of nitrogen dioxide and mortality: a meta-analysis of cohort studies. *Epidemiology (Cambridge, Mass.)*. **29**, 460 (2018)
7. Rai, A.C., et al.: End-user perspective of low-cost sensors for outdoor air pollution monitoring. *Sci. Total Environ.* **607–608**, 691–705 (2017). <https://doi.org/10.1016/j.scitotenv.2017.06.266>
8. European Commission Joint Research Centre: Evaluation of low-cost sensors for air pollution monitoring: effect of gaseous interfering compounds and meteorological conditions. Publications Office, LU (2017)
9. Schneider, P., Castell, N., Vogt, M., Dauge, F.R., Lahoz, W.A., Bartonova, A.: Mapping urban air quality in near real-time using observations from low-cost sensors and model information. *Environ. Int.* **106**, 234–247 (2017). <https://doi.org/10.1016/j.envint.2017.05.005>
10. Kosmopoulos, G., Salamalikis, V., Pandis, S.N., Yannopoulos, P., Bloutsos, A.A., Kazantzidis, A.: Low-cost sensors for measuring airborne particulate matter: field evaluation and calibration at a South-Eastern European site. *Sci. Total Environ.* **748**, 141396 (2020). <https://doi.org/10.1016/j.scitotenv.2020.141396>
11. Giordano, M.R., et al.: From low-cost sensors to high-quality data: a summary of challenges and best practices for effectively calibrating low-cost particulate matter mass sensors. *J. Aerosol Sci.* **158**, 105833 (2021). <https://doi.org/10.1016/j.jaerosci.2021.105833>
12. Zimmerman, N., et al.: A machine learning calibration model using random forests to improve sensor performance for lower-cost air quality monitoring. *Atmos. Meas. Tech.* **11**, 291–313 (2018). <https://doi.org/10.5194/amt-11-291-2018>
13. Jain, S., Presto, A.A., Zimmerman, N.: Spatial modeling of daily PM_{2.5}, NO₂, and CO concentrations measured by a low-cost sensor network: comparison of linear, machine learning, and hybrid land use models. *Environ. Sci. Technol.* **55**, 8631–8641 (2021). <https://doi.org/10.1021/acs.est.1c02653>
14. Landis, M.S., et al.: The U.S. EPA wildland fire sensor challenge: performance and evaluation of solver submitted multi-pollutant sensor systems. *Atmos. Environ.* **247**, 118165 (2021). <https://doi.org/10.1016/j.atmosenv.2020.118165>
15. Barkjohn, K.K., Gantt, B., Clements, A.L.: Development and application of a United States-wide correction for PM_{2.5} data collected with the PurpleAir sensor. *Atmos. Meas. Tech.* **14**, 4617–4637 (2021). <https://doi.org/10.5194/amt-14-4617-2021>
16. Tryner, J., et al.: Laboratory evaluation of low-cost PurpleAir PM monitors and in-field correction using co-located portable filter samplers. *Atmos. Environ.* **220**, 117067 (2020)
17. Masey, N., et al.: Temporal changes in field calibration relationships for Aeroqual S500 O₃ and NO₂ sensor-based monitors. *Sens. Actuators B Chem.* **273**, 1800–1806 (2018). <https://doi.org/10.1016/j.snb.2018.07.087>
18. Malings, C., et al.: Development of a general calibration model and long-term performance evaluation of low-cost sensors for air pollutant gas monitoring. *Atmos. Meas. Tech.* **12**, 903–920 (2019). <https://doi.org/10.5194/amt-12-903-2019>
19. Feenstra, B., et al.: Performance evaluation of twelve low-cost PM_{2.5} sensors at an ambient air monitoring site. *Atmos. Environ.* **216**, 116946 (2019)
20. Christakis, I., Hloupis, G., Stavrakas, I., Tsakiridis, O.: Low cost sensor implementation and evaluation for measuring NO₂ and O₃ pollutants. In: 2020 9th International Conference on Modern Circuits and Systems Technologies (MOCASST), pp. 1–4. IEEE (2020)
21. Mijling, B., Jiang, Q., de Jonge, D., Bocconi, S.: Field calibration of electrochemical NO₂ sensors in a citizen science context. *Atmos. Meas. Tech.* **11**, 1297–1312 (2018). <https://doi.org/10.5194/amt-11-1297-2018>

22. Spinelle, L., Gerboles, M., Aleixandre, M.: Performance evaluation of amperometric sensors for the monitoring of O₃ and NO₂ in ambient air at ppb level. *Procedia Eng.* **120**, 480–483 (2015). <https://doi.org/10.1016/j.proeng.2015.08.676>
23. Dallo, F., et al.: Laboratory calibration and field assessment of low-cost electrochemical Ozone sensors in Alpine and Arctic environments. In: *Geophysical Research Abstracts* (2019)
24. Zuidema, C., Afshar-Mohajer, N., Tatum, M., Thomas, G., Peters, T., Koehler, K.: Efficacy of paired electrochemical sensors for measuring ozone concentrations. *J. Occup. Environ. Hyg.* **16**, 179–190 (2019)
25. Yurko, G., et al.: Real-time sensor response characteristics of 3 commercial metal oxide sensors for detection of BTEX and chlorinated aliphatic hydrocarbon organic vapors. *Chemosensors* **7**, 40 (2019). <https://doi.org/10.3390/chemosensors7030040>
26. Catini, A., et al.: Development of a sensor node for remote monitoring of plants. *Sensors* **19**, 4865 (2019)
27. Marinov, M.B., Ganev, B.T., Nikolov, D.N.: Indoor air quality assessment using low-cost commercial off-the-shelf sensors. In: *2021 6th International Symposium on Environment-Friendly Energies and Applications (EFEA)*, pp. 1–4. IEEE, Sofia, Bulgaria (2021). <https://doi.org/10.1109/EFEA49713.2021.9406260>
28. Hunkeler, U., Truong, H.L., Stanford-Clark, A.: MQTT-S — A publish/subscribe protocol for Wireless Sensor Networks. In: *2008 3rd International Conference on Communication Systems Software and Middleware and Workshops (COMSWARE 2008)*, pp. 791–798. IEEE, Bangalore, India (2008). <https://doi.org/10.1109/COMSWA.2008.4554519>
29. Light, R.A.: Mosquitto: server and client implementation of the MQTT protocol. *J. Open Source Softw.* **2**, 265 (2017). <https://doi.org/10.21105/joss.00265>
30. Nguyen, T.D., Marchal, S., Miettinen, M., Fereidooni, H., Asokan, N., Sadeghi, A.-R.: D²IoT: a federated self-learning anomaly detection system for IoT. In: *2019 IEEE 39th International Conference on Distributed Computing Systems (ICDCS)*, pp. 756–767. IEEE, Dallas, TX, USA (2019). <https://doi.org/10.1109/ICDCS.2019.00080>